Journal of Sound and Vibration (1998) **215**(1), 105–124
Article No. sv981648

NATURAL FREQUENCIES AND MODE SHAPES OF TWO COAXIAL CYLINDRICAL SHELLS COUPLED WITH BOUNDED FLUID

K.-H. JEONG
Korea Atomic Energy Research Institute, *P.O. Box* 105, *Yusong*, *Taejon* 305-600, *Korea*

(*Received* 7 *October* 1997, *and in final form* 2 *March* 1998)

Coaxial shells or cylinders containing fluid have been widely used as structural components in various applications. Several previous investigations have been performed to analyze the free vibration of fluid-filled, coaxial cylindrical shells. However, previous theories were limited to the approximated methods and could provide only the in-phase and out-of-phase modes of coaxial shells with small annular fluid gap compared to the shell diameters. Therefore, the previous theories can only be applicable to the low axial and circumferential modes of coaxial shells with small annular fluid gap. Practically, there exist many ambiguous vibrational modes in addition to the in-phase and out-of-phase modes. In this paper, an advanced general theory is developed which calculates the natural frequencies for all vibrational modes of two coaxial circular cylindrical shells coupled with fluid. To support the validity of the proposed theory, a finite element modal analysis was carried out for the clamped/clamped boundary condition. Excellent agreement was obtained between the analytical solution and the finite element analysis.

1. INTRODUCTION

The free vibration characteristics of fluid-filled coaxial cylindrical shells have been of great concern in the design of reactor internal structures subjected to seismic loadings. Hence, many investigations in this area have been carried out. An analysis of the free vibration of two infinitely long, coaxial cylinders containing fluid has been published by Krajcinovic [1] who separated the fluid loading effect on the cylinders into two terms. The first term is a virtual mass, independent of the flexibility of the other cylinder; the second is a coupling coefficient which is dependent on the flexibility of both cylinders. The author proceeded to solve the equation of motion directly for the coupled natural frequencies, using shell equations for infinitely long cylinders. Chen and Rosenberg [2] derived a frequency equation for two concentrically located circular cylindrical shells containing and separated by incompressible fluid and obtained an approximate closed-form solution. Au-Yang [3] treated the internal structure of a pressurized water reactor as a system of finite coaxial cylinders immersed in a fluid. He estimated the virtual mass and coupling coefficient of two finite cylinders with different lengths immersed in fluid, using the simply supported boundary condition. Finite element methods and experimental investigations of the free vibrational behaviour of coaxial cylinders were conducted by Chiba and Kobayashi [4]. Tani *et al*. [5] performed the free vibration of clamped coaxial cylindrical shells partially filled with incompressible and inviscid liquid. The theoretical analyses were based upon the Galerkin method and the velocity potential theory. Yoshikawa *et al*. [6] studied the vibrational characteristics of a point-driven two concentric submerged

0022–460X/98/310105 + 20 $30.00/0

cylindrical shells, coupled by entrained fluid. The theory on the double shells was based on Flügge's infinite-shell equations. The several complex mixed vibrational modes in the experimental study were reported by Kim *et al*. [7]. However, the incompressible fluid was considered in these theoretical studies, and few theoretical studies on the mixed vibrational modes were taken into consideration. Therefore, this paper attempts to develop an analytical method which calculates the coupled natural frequencies for all vibrational modes of two coaxial cylindrical shells with a fluid-filled annular gap. The clamped boundary condition at both ends of the concentric shells is considered. However, the theory can be extended to any arbitrary classical boundary conditions using an additional simple formulation. This analytical method was verified by FEM.

2. THEORETICAL BACKGROUND

2.1. EQUATION OF MOTION AND BOUNDARY CONDITIONS OF DOUBLE COAXIAL CYLINDRICAL SHELLS

Consider fluid-filled coaxial double cylindrical shells with a clamped boundary condition at both ends, as illustrated in Figure 1. The cylindrical shells have mean radii R_1 and R_2, height L, and wall thickness h. The Sanders' shell equations [8, 9] as the governing equations for both shells where the hydrodynamic effects are considered, can be written as:

$$R_j^2 u_{j,xx} + \frac{(1-\mu)}{2}\left(1+\frac{k_j}{4}\right)u_{j,\theta\theta} + R_j\left\{\frac{(1+\mu)}{2} - \frac{3(1-\mu)}{8}k_j\right\}v_{j,x\theta} + \mu R_j w_{j,x}$$

$$+ \frac{(1-\mu)}{2} R_j k_j w_{j,x\theta\theta} = \gamma_j^2 u_{j,tt}, \tag{1a}$$

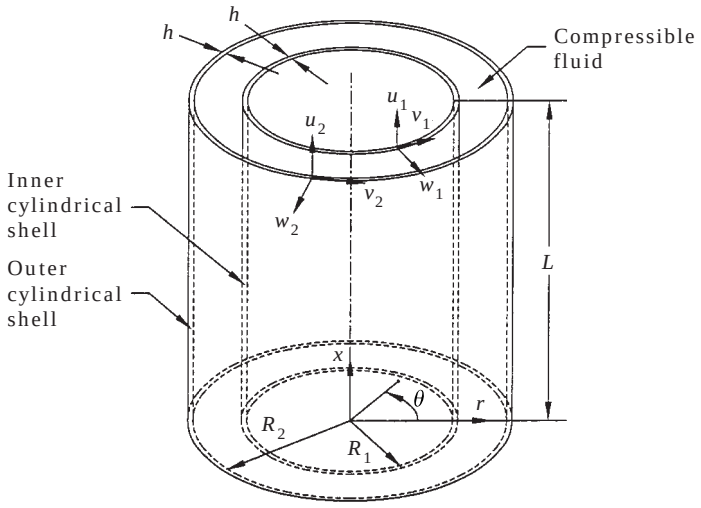

Figure 1. Coaxial cylindrical shells filled with compressible fluid.

$$R_j\left\{\frac{(1+\mu)}{2}-\frac{3(1-\mu)}{8}k_j\right\}u_{j,x\theta}+(1+k_j)v_{j,\theta\theta}+\frac{(1-\mu)}{2}R_j^2\left(1+\frac{9k_j}{4}\right)v_{j,xx}$$

$$-\frac{(3-\mu)}{2}R_j^2k_jw_{j,xx\theta}+w_{j,\theta}-k_jw_{j,\theta\theta\theta}=\gamma_j^2v_{j,tt}, \tag{1b}$$

$$\frac{(1-\mu)}{2}R_jk_ju_{j,x\theta\theta}+\mu R_ju_{j,x}-\frac{(3-\mu)}{2}R_j^2k_jv_{j,xx\theta}+v_{j,\theta}+w_j+k_j(R_j^4w_{j,xxxx}+2R_j^2w_{j,xx\theta\theta}$$

$$+w_{j,\theta\theta\theta\theta}-v_{j,\theta\theta\theta})=-\gamma_j^2w_{j,tt}+\left[\frac{R_j^2p_j}{D}\right], \tag{1c}$$

where the inner shell is referred to with a subscript "1" while the outer shell is denoted by a subscript "2". The comma in the equations denotes a partial derivative with respect to the corresponding variable. For a complete description of the motions of the two concentric cylindrical shells, it is necessary to add boundary conditions to the equations of motion. Consider the simplest end arrangements of the shells on the top and bottom supports. At both ends of two such concentrically arranged shells, the boundary conditions will obviously hold:

$$M_{x1}(0)=N_{x1}(0)=v_1(0)=w_1(0)=0 \quad \text{for the bottom support of the inner shell,} \tag{2a}$$

$$M_{x1}(L)=N_{x1}(L)=v_1(L)=w_1(L)=0 \quad \text{for the top support of the inner shell,} \tag{2b}$$

$$M_{x2}(0)=N_{x2}(0)=v_2(0)=w_2(0)=0 \quad \text{for the bottom support of the outer shell,} \tag{2c}$$

$$M_{x2}(L)=N_{x2}(L)=v_2(L)=w_2(L)=0 \quad \text{for the top support of the outer shell,} \tag{2d}$$

where N_{xj} and M_{xj} denote the membrane tensile force and bending moment, respectively. All geometric boundary conditions applicable to the clamped–clamped shells can be reduced to the following equations at the ends of the inner and outer shells:

$$v_1(0)=w_1(0)=v_2(0)=w_2(0)=0, \tag{3a}$$

$$v_1(L)=w_1(L)=v_2(L)=w_2(L)=0. \tag{3b}$$

The relationships between the forces and displacements are

$$N_{xj}=D\left[u_{j,x}+\frac{\mu}{R_j}v_{j,\theta}+\frac{\mu}{R_j}w_j\right], \tag{4a}$$

$$N_{x\theta j}=\frac{D(1-\mu)}{2}\left[\frac{1}{R_j}(1-\tfrac{3}{4}k_j)u_{j,\theta}+(1+\tfrac{9}{4}k_j)v_{j,x}-3k_jw_{j,x\theta}\right], \tag{4b}$$

$$Q_{xj} = K\left[-\frac{(1-\mu)}{2R_j^3}\, u_{j,\theta\theta} + \frac{(3-\mu)}{2R_j^2}\, v_{j,x\theta} - \frac{(2-\mu)}{R_j^2}\, w_{j,x\theta\theta} - w_{j,xxx} \right], \tag{4c}$$

$$M_{xj} = K\left[\frac{\mu}{R_j^2}\,(v_{j,\theta} - w_{j,\theta\theta}) - w_{j,xx} \right], \tag{4d}$$

where $D = Eh/(1-\mu^2)$, $K = Eh^3/12(1-\mu^2)$, $k_j = h^2/12R_j^2$ and $N_{x\theta j}$, Q_{xj} denote the membrane shear force and transverse shear force, respectively.

2.2. MODAL FUNCTIONS

A general relation for the displacements in any mode of free vibration can be written in the following form for the inner shell $j = 1$ and the outer shell $j = 2$;

$$u_j(x, \theta, t) = u_j(x, \theta)\exp(\mathrm{i}\omega t), \tag{5a}$$

$$v_j(x, \theta, t) = v_j(x, \theta)\exp(\mathrm{i}\omega t), \tag{5b}$$

$$w_j(x, \theta, t) = w_j(x, \theta)\exp(\mathrm{i}\omega t), \qquad j = 1, 2 \tag{5c}$$

where $u_1(x, \theta)$, $v_1(x, \theta)$, $w_1(x, \theta)$, $u_2(x, \theta)$, $v_2(x, \theta)$ and $w_2(x, \theta)$ are modal functions corresponding to the axial, tangential, and radial displacements for the inner and outer shells, respectively. These modal functions along the axial direction can be described by a sum of linear combinations of the Fourier series that are orthogonal.

$$u_j(x, \theta) = \sum_{n=1}^{\infty}\sum_{m=1}^{\infty} A_{mnj}\sin\left(\frac{m\pi x}{L}\right)\cos n\theta, \tag{6a}$$

$$v_j(x, \theta) = \sum_{n=1}^{\infty}\left\{B_{onj} + \sum_{m=1}^{\infty} B_{mnj}\cos\left(\frac{m\pi x}{L}\right)\right\}\sin n\theta, \tag{6b}$$

$$w_j(x, \theta) = \sum_{n=1}^{\infty}\left\{C_{onj} + \sum_{m=1}^{\infty} C_{mnj}\cos\left(\frac{m\pi x}{L}\right)\right\}\cos n\theta, \qquad j = 1, 2. \tag{6c}$$

The modal functions and their derivatives for each shell can be obtained using the finite Fourier transform [9]. The modal functions and their derivatives of the shell are described in reference [8].

2.3. EQUATION OF FLUID MOTION

The inviscid, irrotational and compressible fluid movement due to shell vibration is described by the general velocity potential equation:

$$\Phi_{,rr} + \frac{1}{r}\Phi_{,r} + \frac{1}{r^2}\Phi_{,\theta\theta} + \Phi_{,xx} = \frac{1}{c^2}\Phi_{,tt}, \tag{7}$$

where c is the speed of sound in the fluid medium equal to $\sqrt{B/\rho_o}$, B is the bulk modulus of elasticity of fluid and ρ_o stands for the fluid density. It is possible to separate the function Φ with respect to x by observing that, in the axial direction, the rigid surfaces support the edges of the shells; thus

$$\Phi(x, r, \theta, t) = \mathrm{i}\omega\phi(r, \theta, x)\exp(\mathrm{i}\omega t) = \mathrm{i}\omega\eta(r, \theta)f(x)\exp(\mathrm{i}\omega t), \qquad \mathrm{i} = \sqrt{-1}, \tag{8}$$

where ω is the coupled frequency of the shells. Substitution of equation (8) into the partial differential equation (7) gives

$$\frac{\left[\eta(r, \theta)_{,rr} + \frac{1}{r}\eta(r, \theta)_{,r} + \frac{1}{r^2}\eta(r, \theta)_{,\theta\theta} + \left(\frac{\omega}{c}\right)^2 \eta(r, \theta)\right]}{\eta(r, \theta)} = -\frac{f(x)_{,xx}}{f(x)} = \left(\frac{m\pi}{L}\right)^2. \tag{9}$$

It is possible to solve the partial differential equation (9) by the separation of the variables technique,

$$\phi(x, \theta, r) = \sum_{n=1}^{\infty}\left[\begin{array}{c} D_{on1}J_n\left(\frac{\omega}{c}\right) + D_{on2}Y_n\left(\frac{\omega}{c}r\right) \\ + \sum_{m=1}^{\infty}\left[D_{mn1}I_n(\alpha_{mn}r) + D_{mn2}K_n(\alpha_{mn}r)\right]\cos\left(\frac{m\pi x}{L}\right) \end{array}\right]\sin n\theta,$$

$$\text{for} \quad \frac{m\pi}{L} \geqslant \frac{\omega}{c} \tag{10a}$$

and

$$\phi(x, \theta, r) = \sum_{n=1}^{\infty}\left[\begin{array}{c} D_{on1}J_n\left(\frac{\omega}{c}r\right) + D_{on2}Y_n\left(\frac{\omega}{c}r\right) \\ + \sum_{m=1}^{\infty}\left[D_{mn1}J_n(\alpha_{mn}r) + D_{mn2}Y_n(\alpha_{mn}r)\right]\cos\left(\frac{m\pi x}{L}\right) \end{array}\right]\sin n\theta,$$

$$\text{for} \quad \frac{m\pi}{L} < \frac{\omega}{c}, \tag{10b}$$

where J_n and Y_n are Bessel functions of the first and second kinds of order n, whereas I_n and K_n are modified Bessel functions of the first and second kinds of order n. ϕ means the spacial velocity potential for the contained fluid and α_{mn} is related to the speed of sound in the fluid medium.

$$\alpha_{mn} = \sqrt{\left|\left(\frac{m\pi}{L}\right)^2 - \left(\frac{\omega}{c}\right)^2\right|}, \quad \text{for } m = 1, 2, 3, \ldots. \tag{11}$$

The boundary conditions of velocity potential ϕ appear as follows:

(1) impermeable rigid surfaces on the bottom

$$\phi(0, \theta, r)_{,x} = 0; \tag{12}$$

(2) as there exists no free surface, the axial velocity of fluid at the rigid shell top is also zero, so

$$\phi(L, \theta, r)_{,x} = 0; \tag{13}$$

(3) the radial fluid velocity along the outer wetted surface of the inner shell must be identical to the radial velocity of the flexible shell, so

$$\phi(x, \theta, R_1)_{,r} = w_1(x, \theta); \tag{14}$$

(4) the radial fluid velocity along the inner wetted surface of the outer shell must be identical to the radial velocity of the shell, so

$$\phi(x, \theta, R_2)_{,r} = w_2(x, \theta). \tag{15}$$

Substituting equation (6c), (10a) and (10b) into equations (14) and (15) gives the relationships, not only between C_{onj} and D_{onj}, but also C_{mnj} and D_{mnj}:

$$\sum_{n=1}^{\infty}\left[\begin{array}{c}\left(\frac{\omega}{c}\right)D_{on1}J_n'\left(\frac{\omega}{c}R_1\right)+\left(\frac{\omega}{c}\right)D_{on2}Y_n'\left(\frac{\omega}{c}R_1\right)\\ +\sum_{m=1}^{\infty}\left\{\alpha_{mn}[D_{mn1}I_n'(\alpha_{mn}R_1)+D_{mn2}K_n'(\alpha_{mn}R_1)]\cos\left(\frac{m\pi x}{L}\right)\right\}\end{array}\right]\cos n\theta$$

$$=\sum_{n=1}^{\infty}\left[C_{on1}+\sum_{m=1}^{\infty}C_{mn1}\cos\left(\frac{m\pi x}{L}\right)\right]\cos n\theta, \qquad \text{for} \quad \frac{m\pi}{L}\geqslant\frac{\omega}{c}, \tag{16a}$$

$$\sum_{n=1}^{\infty}\left[\begin{array}{c}\left(\frac{\omega}{c}\right)D_{on1}J_n'\left(\frac{\omega}{c}R_2\right)+\left(\frac{\omega}{c}\right)D_{on2}Y_n'\left(\frac{\omega}{c}R_2\right)\\ +\sum_{m=1}^{\infty}\left\{\alpha_{mn}[D_{mn1}I_n'(\alpha_{mn}R_2)+D_{mn2}K_n'(\alpha_{mn}R_2)]\cos\left(\frac{m\pi x}{L}\right)\right\}\end{array}\right]\cos n\theta$$

$$=\sum_{n=1}^{\infty}\left[C_{on2}+\sum_{m=1}^{\infty}C_{mn2}\cos\left(\frac{m\pi x}{L}\right)\right]\cos n\theta, \qquad \text{for} \quad \frac{m\pi}{L}\geqslant\frac{\omega}{c}, \tag{16b}$$

Now, equation (16) will be reduced to

$$\left(\frac{\omega}{c}\right)\begin{bmatrix} J_n'\left(\frac{\omega}{c}R_1\right) & Y_n'\left(\frac{\omega}{c}R_1\right) \\ J_n'\left(\frac{\omega}{c}R_2\right) & Y_n'\left(\frac{\omega}{c}R_2\right) \end{bmatrix}\begin{Bmatrix} D_{on1} \\ D_{on2} \end{Bmatrix} = \begin{Bmatrix} C_{on1} \\ C_{on2} \end{Bmatrix}, \tag{17a}$$

$$\alpha_{mn}\begin{bmatrix} I_n'(\alpha_{mn}R_1) & K_n'(\alpha_{mn}R_1) \\ I_n'(\alpha_{mn}R_2) & K_n'(\alpha_{mn}R_2) \end{bmatrix}\begin{Bmatrix} D_{mn1} \\ D_{mn2} \end{Bmatrix} = \begin{Bmatrix} C_{mn1} \\ C_{mn2} \end{Bmatrix}. \tag{17b}$$

When $m\pi/L < \omega/c$, $I_n'(\,)$ and $K_n'(\,)$ in equations (16a), (16b) and (17b) should be replaced by $J_n'(\,)$ and $Y_n'(\,)$, respectively. When the hydrostatic pressures on the shells are neglected, the hydrodynamic pressures along the inner and outer wetted shell surfaces can be given by

$$p_j(x, \theta, t) = \delta_j \rho_o \omega^2 \phi(x, \theta, R_j) \exp(\mathrm{i}\omega t), \tag{18}$$

where $\delta_j = 1$ for $j = 1$ and $\delta_j = -1$ for $j = 2$. Finally, the hydrodynamic forces on the inner and outer shells can be written as

$$\frac{R_j^2 p_j(x, \theta, t)}{D} = \frac{\rho_o \omega^2 R_j^2 \delta_j}{D} \sum_{n=1}^{\infty} \left\{ C_{on1}\Gamma_{onj} + C_{on2}G_{onj} + \sum_{m=1}^{\infty} [C_{mn1}\Gamma_{mnj} + C_{mn2}G_{mnj}] \cos\left(\frac{m\pi x}{L}\right) \right\} \sin n\theta \exp(\mathrm{i}\omega t). \tag{19}$$

2.4. GENERAL FORMULATION

The dynamic displacements and their derivatives may be represented by a Fourier sine and cosine series in an open range of $0 < x < L$ and with the end values using the finite Fourier transform [8]. Substitution of the displacements and their derivatives into the governing Sanders' shell equations (1a), (1b) and (1c), leads to an explicit relation for B_{onj}, C_{onj}, and a set of equations for A_{mnj}, B_{mnj}, C_{mnj}, as follows:

$$B_{onj} = q_{1j}(u_j^o + u_j^L) + q_{2j}(\tilde{v}_j^o + \tilde{v}_j^L) + q_{3j}(\tilde{w}_j^o + \tilde{w}_j^L) + q_{4j}(\tilde{\tilde{w}}_j^o + \tilde{\tilde{w}}_j^L), \tag{20}$$

$$C_{onj} = q_{5j}(u_j^o + u_j^L) + q_{6j}(\tilde{v}_j^o + \tilde{v}_j^L) + q_{7j}(\tilde{w}_j^o + \tilde{w}_j^L) + q_{8j}(\tilde{\tilde{w}}_j^o + \tilde{\tilde{w}}_j^L), \tag{21}$$

$$\begin{bmatrix} d_{11} & d_{12} & d_{13} & 0 & 0 & 0 \\ d_{12} & d_{22} & d_{23} & 0 & 0 & 0 \\ d_{13} & d_{23} & d_{33} & 0 & 0 & d_{63} \\ 0 & 0 & 0 & d_{44} & d_{45} & d_{46} \\ 0 & 0 & 0 & d_{45} & d_{55} & d_{56} \\ 0 & 0 & d_{36} & d_{46} & d_{56} & d_{66} \end{bmatrix} \begin{bmatrix} A_{mn1} \\ B_{mn1} \\ C_{mn1} \\ A_{mn2} \\ B_{mn2} \\ C_{mn2} \end{bmatrix}$$

$$= \begin{bmatrix} -a_{11}m[u_1^o + (-1)^m u_1^L] \\ a_{12}[u_1^o + (-1)^m u_1^L] + a_{13}[\tilde{v}_1^o + (-1)^m \tilde{v}_1^L] + a_{14}[\tilde{w}_1^o + (-1)^m \tilde{w}_1^L] \\ a_{15}[u_1^o + (-1)^m u_1^L] + a_{14}[\tilde{v}_1^o + (-1)^m \tilde{v}_1^L] + a_{18}[\tilde{w}_1^o + (-1)^m \tilde{w}_1^L] + a_{19}[\tilde{\tilde{w}}_1^o + (-1)^m \tilde{\tilde{w}}_1^L - m^2 \tilde{w}_1^o - m^2 (-1)^m \tilde{w}_1^L] \\ -a_{21}m[u_2^o + (-1)^m u_2^L] \\ a_{22}[u_2^o + (-1)^m u_2^L] + a_{23}[\tilde{v}_2^o + (-1)^m \tilde{v}_2^L] + a_{24}[\tilde{w}_2^o + (-1)^m \tilde{w}_2^L] \\ a_{25}[u_2^o + (-1)^m u_2^L] + a_{24}[\tilde{v}_2^o + (-1)^m \tilde{v}_2^L] + a_{28}[\tilde{w}_2^o + (-1)^m \tilde{w}_2^L] + a_{29}[\tilde{\tilde{w}}_2^o + (-1)^m \tilde{\tilde{w}}_2^L - m^2 \tilde{w}_2^o - m^2 (-1)^m \tilde{w}_2^L] \end{bmatrix} \tag{22}$$

where the end values in equation (20)–(22) are defined as

$$u_j^o = -\frac{2u_j(0,\theta)}{\pi\cos n\theta}, \qquad u_j^L = \frac{2u_j(L,\theta)}{\pi\cos n\theta}, \qquad \tilde{v}_j^o = -\frac{2Lv_{j,x}(0,\theta)}{\pi^2\sin n\theta}, \qquad \tilde{v}_j^L = \frac{2Lv_{j,x}(L,\theta)}{\pi^2\sin n\theta},$$

$$\tilde{w}_j^o = -\frac{2Lw_{j,x}(0,\theta)}{\pi^2\cos n\theta}, \qquad \tilde{w}_j^L = \frac{2Lw_{j,x}(L,\theta)}{\pi^2\cos n\theta}, \qquad \tilde{\tilde{w}}_j^o = -\frac{2L^3w_{j,xxx}(0,\theta)}{\pi^4\cos n\theta},$$

$$\tilde{\tilde{w}}_j^L = \frac{2L^3w_{j,xxx}(L,\theta)}{\pi^4\cos n\theta}. \tag{23}$$

The equivalent hydrodynamic mass effect on the inner shell is included in the coefficient d_{33}, and the effect on the outer shell is contained in the coefficient d_{66}. The coefficient d_{36} indicates the equivalent hydraulic pressure on the inner shell induced by the outer shell motion, and similarly d_{63} stands for the equivalent hydraulic pressure on the outer shell induced by the inner shell motion. Generally speaking, the coefficient $d_{36} \neq d_{63}$. Therefore the matrix equation (22) is asymmetric. The matrix equation is coupled by two coefficient terms d_{36} and d_{63}.

The forces $N_{x\theta j}$ and Q_{xj} at the ends of the shells can be written as a combination of some boundary values of displacement and their derivatives using equation (3).

$$N_{x\theta j}(0,\theta) = [f_{1j}u_j^o + f_{2j}\tilde{v}_j^o + f_{3j}\tilde{w}_j^o]\sin n\theta, \tag{24a}$$

$$N_{x\theta j}(L,\theta) = -[f_{1j}u_j^L + f_{2j}\tilde{v}_j^L + f_{3j}\tilde{w}_j^L]\sin n\theta, \tag{24b}$$

$$Q_{xj}(0,\theta) = [f_{4j}u_j^o + f_{5j}\tilde{v}_j^o + f_{6j}\tilde{w}_j^o + f_{7j}\tilde{\tilde{w}}_j^o]\cos n\theta, \tag{24c}$$

$$Q_{xj}(L,\theta) = -[f_{4j}u_j^L + f_{5j}\tilde{v}_j^L + f_{6j}\tilde{w}_j^L + f_{7j}\tilde{\tilde{w}}_j^L]\cos n\theta, \tag{24d}$$

where f_{ij} $(i = 1, 2, \ldots, 7,\ j = 1, 2)$ are the derived coefficients. The boundary values of displacement and their derivatives, $\tilde{v}_j^o$, $\tilde{v}_j^L$, $\tilde{\tilde{w}}_j^o$ and $\tilde{\tilde{w}}_j^L$ can be transformed in a combination of the boundary values of u_j, $\tilde{w}_j$, $N_{x\theta j}$ and Q_{xj} by equation (4), as written in the form

$$\tilde{v}_j^o = [g_{1j}u_j^o + g_{2j}\tilde{w}_j^o + g_{3j}N_{x\theta_j^o}], \tag{25a}$$

$$\tilde{v}_j^L = [g_{1j}u_j^L + g_{2j}\tilde{w}_j^L + g_{3j}N_{x\theta_j^L}], \tag{25b}$$

$$\tilde{\tilde{w}}_j^o = [g_{4j}u_j^o + g_{5j}\tilde{w}_j^o + g_{6j}N_{x\theta_j^o} + g_{7j}Q_{x_j^o}], \tag{25c}$$

$$\tilde{\tilde{w}}_j^L = [g_{4j}u_j^L + g_{5j}\tilde{w}_j^L + g_{6j}N_{x\theta_j^L} + g_{7j}Q_{x_j^L}], \tag{25d}$$

where

$$N_{x\theta_j^o} = \frac{N_{x\theta j}(0,\theta)}{\sin n\theta}, \qquad N_{x\theta_j^L} = -\frac{N_{x\theta j}(L,\theta)}{\sin n\theta}, \qquad Q_{x_j^o} = \frac{Q_{xj}(0,\theta)}{\cos n\theta},$$

$$Q_{x_j^L} = -\frac{Q_{xj}(L,\theta)}{\cos n\theta}, \tag{26}$$

g_{ij} $(i = 1, 2, \ldots, 7,\ j = 1, 2)$ can also be derived.

Substitution of equation (25) into equations (20), (21) and (22) gives

$$B_{on1} = \sum_{j=1}^{2} [\beta_{1j}(u_j^o + u_j^L) + \beta_{2j}(\tilde{w}_j^o + \tilde{w}_j^L) + \beta_{3j}(N_{x\theta_j^o} + N_{x\theta_j^L}) + \beta_{4j}(Q_{x_j^o} + Q_{x_j^L})], \tag{27a}$$

$$B_{on2} = \sum_{j=1}^{2} [\beta_{5j}(u_j^o + u_j^L) + \beta_{6j}(\tilde{w}_j^o + \tilde{w}_j^L) + \beta_{7j}(N_{x\theta_j^o} + N_{x\theta_j^L}) + \beta_{8j}(Q_{x_j^o} + Q_{x_j^L})], \tag{27b}$$

$$C_{on1} = \sum_{j=1}^{2} [\delta_{1j}(u_j^o + u_j^L) + \delta_{2j}(\tilde{w}_j^o + \tilde{w}_j^L) + \delta_{3j}(N_{x\theta_j^o} + N_{x\theta_j^L}) + \delta_{4j}(Q_{x_j^o} + Q_{x_j^L})] \tag{27c}$$

$$C_{on2} = \sum_{j=1}^{2} [\delta_{5j}(u_j^o + u_j^L) + \delta_{6j}(\tilde{w}_j^o + \tilde{w}_j^L) + \delta_{7j}(N_{x\theta_j^o} + N_{x\theta_j^L}) + \delta_{8j}(Q_{x_j^o} + Q_{x_j^L})], \tag{27d}$$

$$\begin{bmatrix} A_{mn1} \\ B_{mn1} \\ C_{mn1} \\ A_{mn2} \\ B_{mn2} \\ C_{mn2} \end{bmatrix} = [\zeta] \begin{bmatrix} \{u_1^o + (-1)^m u_1^L\} \\ \{u_2^o + (-1)^m u_2^L\} \\ \{\tilde{w}_1^o + (-1)^m \tilde{w}_1^L\} \\ \{\tilde{w}_2^o + (-1)^m \tilde{w}_2^L\} \\ \{N_{x\theta_1^o} + (-1)^m N_{x\theta_1^L}\} \\ \{N_{x\theta_2^o} + (-1)^m N_{x\theta_2^L}\} \\ \{Q_{x_1^o} + (-1)^m Q_{x_1^L}\} \\ \{Q_{x_2^o} + (-1)^m Q_{x_2^L}\} \end{bmatrix}, \tag{28}$$

where β_{ij} and δ_{ij} in equation (27) are the derived coefficients, and $[\zeta]$ in equation (28) is the 8×6 derived coefficients matrix. Eventually, all Fourier coefficients A_{mnj}, B_{mnj} and C_{mnj} are rearranged with a combination of the end point values, as shown in equation (28).

The geometric boundary conditions that must be satisfied are associated with displacements v_j and w_j. Hence, it follows that

$$v_1(0) = \sum_{n=1}^{\infty} \left[B_{on1} + \sum_{m=1}^{\infty} B_{mn1} \right] = 0, \qquad v_1(L) = \sum_{n=1}^{\infty} \left[B_{on1} + \sum_{m=1}^{\infty} B_{mn1}(-1)^m \right] = 0, \tag{29a, b}$$

$$v_2(0) = \sum_{n=1}^{\infty} \left[B_{on2} + \sum_{m=1}^{\infty} B_{mn2} \right] = 0, \qquad v_2(L) = \sum_{n=1}^{\infty} \left[B_{on2} + \sum_{m=1}^{\infty} B_{mn2}(-1)^m \right] = 0, \tag{29c, d}$$

$$w_1(0) = \sum_{n=1}^{\infty}\left[C_{on1} + \sum_{m=1}^{\infty} C_{mn1}\right] = 0, \qquad w_1(L) = \sum_{n=1}^{\infty}\left[C_{on1} + \sum_{m=1}^{\infty} C_{mn1}(-1)^m\right] = 0,$$

(29e, f)

$$w_2(0) = \sum_{n=1}^{\infty}\left[C_{on2} + \sum_{m=1}^{\infty} C_{mn2}\right] = 0, \qquad w_2(L) = \sum_{n=1}^{\infty}\left[C_{on2} + \sum_{m=1}^{\infty} C_{mn2}(-1)^m\right] = 0.$$

(29g, h)

Substitution of equations (27) and (28) for the coefficients B_{onj}, C_{onj}, A_{mnj}, B_{mnj} and C_{mnj} into the eight constraint conditions which come from the geometric boundary condition, written as equation (29), leads to a homogeneous matrix equation:

$$\begin{bmatrix}
e_{11} & e_{12} & e_{13} & e_{14} & e_{15} & e_{16} & e_{17} & e_{18} & c_{11} & c_{12} & c_{13} & c_{14} & c_{15} & c_{16} & c_{17} & c_{18} \\
e_{12} & e_{11} & e_{14} & e_{13} & e_{16} & e_{15} & e_{18} & e_{17} & c_{12} & c_{11} & c_{14} & c_{13} & c_{16} & c_{15} & c_{18} & c_{17} \\
e_{21} & e_{22} & e_{23} & e_{24} & e_{25} & e_{26} & e_{27} & e_{28} & c_{21} & c_{22} & c_{23} & c_{24} & c_{25} & c_{26} & c_{27} & c_{28} \\
e_{22} & e_{21} & e_{24} & e_{23} & e_{26} & e_{25} & e_{28} & e_{27} & c_{22} & c_{21} & c_{24} & c_{23} & c_{26} & c_{25} & c_{28} & c_{27} \\
e_{31} & e_{32} & e_{33} & e_{34} & e_{35} & e_{36} & e_{37} & e_{38} & c_{31} & c_{32} & c_{33} & c_{34} & c_{35} & c_{36} & c_{37} & c_{38} \\
e_{32} & e_{31} & e_{34} & e_{33} & e_{36} & e_{35} & e_{38} & e_{37} & c_{32} & c_{31} & c_{34} & c_{33} & c_{36} & c_{35} & c_{38} & c_{37} \\
e_{41} & e_{42} & e_{43} & e_{44} & e_{45} & e_{46} & e_{47} & e_{48} & c_{41} & c_{42} & c_{43} & c_{44} & c_{45} & c_{46} & c_{47} & c_{48} \\
e_{42} & e_{41} & e_{44} & e_{43} & e_{46} & e_{45} & e_{48} & e_{47} & c_{42} & c_{41} & c_{44} & c_{43} & c_{46} & c_{45} & c_{48} & c_{47}
\end{bmatrix}$$

$$\times [H] = \{0\}, \qquad (30)$$

$$[H] = [u_1^o \quad u_1^L \quad u_2^o \quad u_2^L \quad \tilde{w}_1^L \quad \tilde{w}_1^L \quad \tilde{w}_2^o \quad \tilde{w}_2^L \quad N_{x\theta_1^o}$$

$$N_{x\theta_1^L} \quad N_{x\theta_2^o} \quad N_{x\theta_2^L} \quad Q_{x_1^o} \quad Q_{x_1^L} \quad Q_{x_2^o} \quad Q_{x_2^L}]^T. \qquad (31)$$

The elements of the matrix, e_{ik} and c_{ik} ($i = 1, 2, \ldots, 4$ and $k = 1, 2, \ldots, 8$) can be obtained from equation (29). However, when both cylindrical shells are clamped at both support ends, the associated boundary conditions are

$$u_j = 0, \qquad v_j = 0, \qquad w_j = 0, \qquad w_{j,x} = 0 \quad \text{at} \quad x = 0 \quad \text{and} \quad L. \qquad (32)$$

Among these boundary conditions, the two geometric boundary conditions $u_1 = 0$, $u_2 = 0$, $\tilde{w}_1 = 0$ and $\tilde{w}_2 = 0$ at $x = 0$ and $x = L$ are not automatically satisfied by equation (5), the modal functions set. Therefore the first, second, third, and fourth rows of the matrix in equation (30) are enforced and the terms associated with u_j^o, u_j^L, $\tilde{w}_j^o$ and $\tilde{w}_j^L$ are released. The 8×8 frequency determinant is obtained from equation (30) by retaining the rows and

columns associated with $N_{x\theta_j^o}$, $N_{x\theta_j^L}$, $Q_{x_j^o}$ and $Q_{x_j^L}$. For the clamped boundary condition, the coupled natural frequencies are numerically obtained from the frequency determinant:

$$\begin{vmatrix} c_{11} & c_{12} & c_{13} & c_{14} & c_{15} & c_{16} & c_{17} & c_{18} \\ c_{12} & c_{11} & c_{14} & c_{13} & c_{16} & c_{15} & c_{18} & c_{17} \\ c_{21} & c_{22} & c_{23} & c_{24} & c_{25} & c_{26} & c_{27} & c_{28} \\ c_{22} & c_{21} & c_{24} & c_{23} & c_{26} & c_{25} & c_{28} & c_{27} \\ c_{31} & c_{32} & c_{33} & c_{34} & c_{35} & c_{36} & c_{37} & c_{38} \\ c_{32} & c_{31} & c_{34} & c_{33} & c_{36} & c_{35} & c_{38} & c_{37} \\ c_{41} & c_{42} & c_{43} & c_{44} & c_{45} & c_{46} & c_{47} & c_{48} \\ c_{42} & c_{41} & c_{44} & c_{43} & c_{46} & c_{45} & c_{48} & c_{47} \end{vmatrix} = 0. \tag{33}$$

3. EXAMPLE AND DISCUSSION

3.1. FEM MODEL AND CONVERGENCE TEST

On the basis of the preceding analysis, the frequency determinant is numerically solved for the clamped boundary condition in order to find the coupled natural frequencies of the coaxial double cylindrical shells filled with bounded compressible fluid. The inner and outer shells are coupled with a fluid-filled annular gap. In order to check the validity and accuracy of the results from the theoretical study and compare them to the FEM result, computation is carried out for the fluid-coupled system. The inner cylindrical shell has a mean radius of 100 mm, a length of 300 mm, and a wall thickness of 2 mm. The outer cylindrical shell has a mean radius of 150 mm with the same length and wall thickness. The physical properties of the shell material are as follows: Young's modulus = 69·0 GPa, Poisson's ratio = 0·3, and mass density = 2700 kg/m^3. Water is used as the contained fluid, having a density of 1000 kg/m^3. The sound speed in water, 1483 m/s, is equivalent to the bulk modulus of elasticity, 2·2 GPa. The clamped boundary condition at both ends of the two shells is considered.

The frequency equation derived in the preceding section involves an infinite series of algebraic terms. Before exploring the analytical method to obtain the coupled natural frequencies of the fluid-coupled shells, it is necessary to conduct convergence studies and establish the number of terms which are required in the series expansions involved. In the numerical calculation, the Fourier expansion term m is set at 100, which gives an exact enough solution by convergence. In general, the solution approaches the exact frequency from above as the number of terms included in the series increases. However, the use of more than 100 terms does not improve the solutions significantly. Finite element analyses using a commercial computer code ANSYS software (version 5.2) are performed to verify the results of the theoretical study. The FEM results are used as the baseline data. In the finite elements analysis, two-dimensional axisymmetric models are constructed with axisymmetric two-dimensional fluid elements (FLUID81) and axisymmetric shell elements (SHELL61). The fluid region is divided into a number of identical fluid elements with four nodes. The circular cylindrical shell is modelled as deformable shell elements with two nodes. The fluid boundary conditions at the top and bottom of the tank are zero displacement and rotations. The nodes which are connected entirely by the fluid elements are free to move arbitrarily in three-dimensional space, with the exception of those which

are restricted to motion in the bottom and top surfaces of the fluid cavity. The radial velocities of the fluid nodes along the wetted shell surfaces are coincided to the corresponding velocities of the shells. The FEM model has 320 (radially 8 × axially 40) fluid elements and 80 shell elements. The inner and outer shells each consist of 40 identical shell elements.

3.2. VERIFICATION OF THE ANALYTICAL METHOD

Table 1 will make it easier to check the accuracy of the frequencies and compare the theoretical frequencies with the corresponding FEM ones. The discrepancy is defined as

$$\text{Discrepancy}(\%) = \frac{(\text{frequency obtained by FEM} - \text{theoretical frequency})}{\text{frequency obtained by FEM}} \times 100. \quad (34)$$

TABLE 1

Coupled natural frequencies (Hz) of the fluid-filled coaxial shells

Serial mode	Apparent mode		Coupled frequency		Mode phase	Discrepancy (%)
	n	m'	FEM	theory		
1	1	1	392·0	391·1	out-of-phase	0·23
2	1	2	856·6	847·6	out-of-phase	1·05
3	1	3	1417·8	1397·5	out-of-phase	1·43
4	1	1	1735·7	1736·6	in-phase	−0·05
5	1	4	1939·1	1908·5	out-of-phase	1·57
6	1	5	2359·8	2317·2	out-of-phase	1·81
7	1	–	2604·2	2623·4	mixed phase	−0·74
1	2	1	434·8	435·6	out-of-phase	−0·18
2	2	2	909·7	907·1	out-of-phase	0·28
3	2	1	994·1	996·8	in-phase	−0·27
4	2	3	1414·6	1401·3	out-of-phase	0·94
5	2	–	1828·0	1822·2	mixed phase	0·32
6	2	–	1911·8	1892·6	mixed phase	1·00
7	2	–	2302·1	2265·3	mixed phase	1·60
1	3	1	402·2	403·0	out-of-phase	−0·20
2	3	1	669·2	671·3	in-phase	−0·31
3	3	2	858·3	858·3	out-of-phase	0·00
4	3	2	1341·4	1344·8	in-phase	−0·25
5	3	3	1359·3	1352·4	out-of-phase	0·51
6	3	4	1829·5	1810·7	out-of-phase	1·03
7	3	3	2012·0	2010·6	in-phase	0·07
1	4	1	382·1	382·5	out-of-phase	−0·10
2	4	1	559·9	561·9	in-phase	−0·36
3	4	2	790·6	791·0	out-of-phase	0·05
4	4	2	1072·0	1075·5	in-phase	−0·32
5	4	3	1271·2	1267·5	out-of-phase	0·29
6	4	3	1674·5	1676·9	in-phase	−0·14
7	4	4	1742·2	1729·2	out-of-phase	0·76
1	5	1	385·5	385·6	out-of-phase	0·02
2	5	1	655·4	658·4	in-phase	−0·46
3	5	2	748·5	748·5	out-of-phase	0·00
4	5	2	1005·2	1008·9	in-phase	−0·37
5	5	3	1194·1	1191·5	out-of-phase	0·22
6	5	3	1512·3	1515·9	in-phase	0·23
7	5	4	1658·0	1648·2	out-of-phase	0·59
8	5	4	2087·9	2086·8	in-phase	0·05

The largest discrepancies between the theoretical and FEM results are 1·81% for the circumferential wavenumber, $n = 1$, and the apparent axial mode number, $m' = 4$, and 1·60% for $n = 2$ with the seventh serial mode. Discrepancies defined by equation (34) are always less than 2% and their root mean square is about 0·7%. As the coarse mesh of the FEM model changes to fine mesh, all natural frequencies may approach the theoretical results. As may be seen, the present results agree quite well with FEM solution.

3.3. MODE SHAPES

Mode shapes of the fluid-coupled coaxial double shells are obtained by the FEM and plotted in Figures 2–4. The dashed lines in the figures represent the undeformed shapes of the two-dimensional cylindrical shells. Figures 2–4 show the deformed mode shapes of the fluid and shell elements for the circumferential wavenumber $n = 1$, 2 and 3, respectively. Note that the co-ordinate axial symbols in the figures indicate the axis of the shells at $x = 0$. In the higher axial mode numbers of the vibrational mode shapes, the separations between the two-dimensional axisymmetric cylindrical shells and fluid regions appear because only a radial coupling on the shell–fluid interface is applied in the FEM simulation. The radial coupling is assured by equations (14) and (15) in the theory. Practically, in the real fluid, the separations between the shells and fluid regions cannot appear because of the boundary layer due to fluid damping. However, if the perfect coupling, including the axial and azimuthal directions, is simulated in the FEM model, the movement of fluid elements in contact with the shell elements is restricted to the axial and azimuthal directions. It will not be realistic for the light damping fluid or non-viscous fluid. The perfect coupling between the shells and the contained fluid in the FEM simulation can produce some errors which will exaggerate the added mass effect and underestimate the coupled frequencies. In the FEM simulation model, the slips towards the axial and azimuthal directions along the surface of the shell–fluid interface should be preserved instead of the perfect coupling for more realistic physical phenomena. The little separations between them may not be significant because all the mode shapes in Figures 2–4 are exaggerated, compared to the vibrational amplitudes of real linear free vibration. In order to compensate the separation phenomena between the shell and fluid, the assumption that the radial fluid velocity should be identical to the radial shell velocity along the fluid-contacting surfaces, must be changed to the realistic physical phenomena. That is to say, the fluid velocity along the contacting surfaces must always be normal to the shell surface during vibration. The realistic boundary condition may lead to a non-linear boundary equation. Eventually it will provide a complex theoretical model. As the number of the axial and circumferential modes increases, the separation will arise in a wide range except the anti-nodes and it will overestimate the coupled natural frequencies.

All of the mode shapes can be classified into three mode categories according to the relative moving directions between the inner and outer shells during vibration: in-phase mode, out-of-phase mode, and mixed modes. The vibrational mode shapes show some ambiguous vibrational modes, neither apparent in-phase modes nor apparent out-of-phase modes, which are now called *mixed vibrational modes*. When two parallel identical cylinders are submerged in an ideal fluid, there exist only the in-phase and out-of-phase vibrational modes, as shown in section 3.2 of reference [10]. On the other hand, as the two coaxial circular cylindrical shells cannot have the same diameter although they have the same length, their mode shapes in vacuum cannot be exactly identical. As the two coaxial circular cylindrical shells vibrate independently in vacuum, they will have different natural frequencies and mode shapes for the corresponding mode numbers. When the annulus between the shells is filled with a low-density fluid, they will still maintain the different natural frequencies and mode shapes by a weak fluid coupling effect. As the fluid density

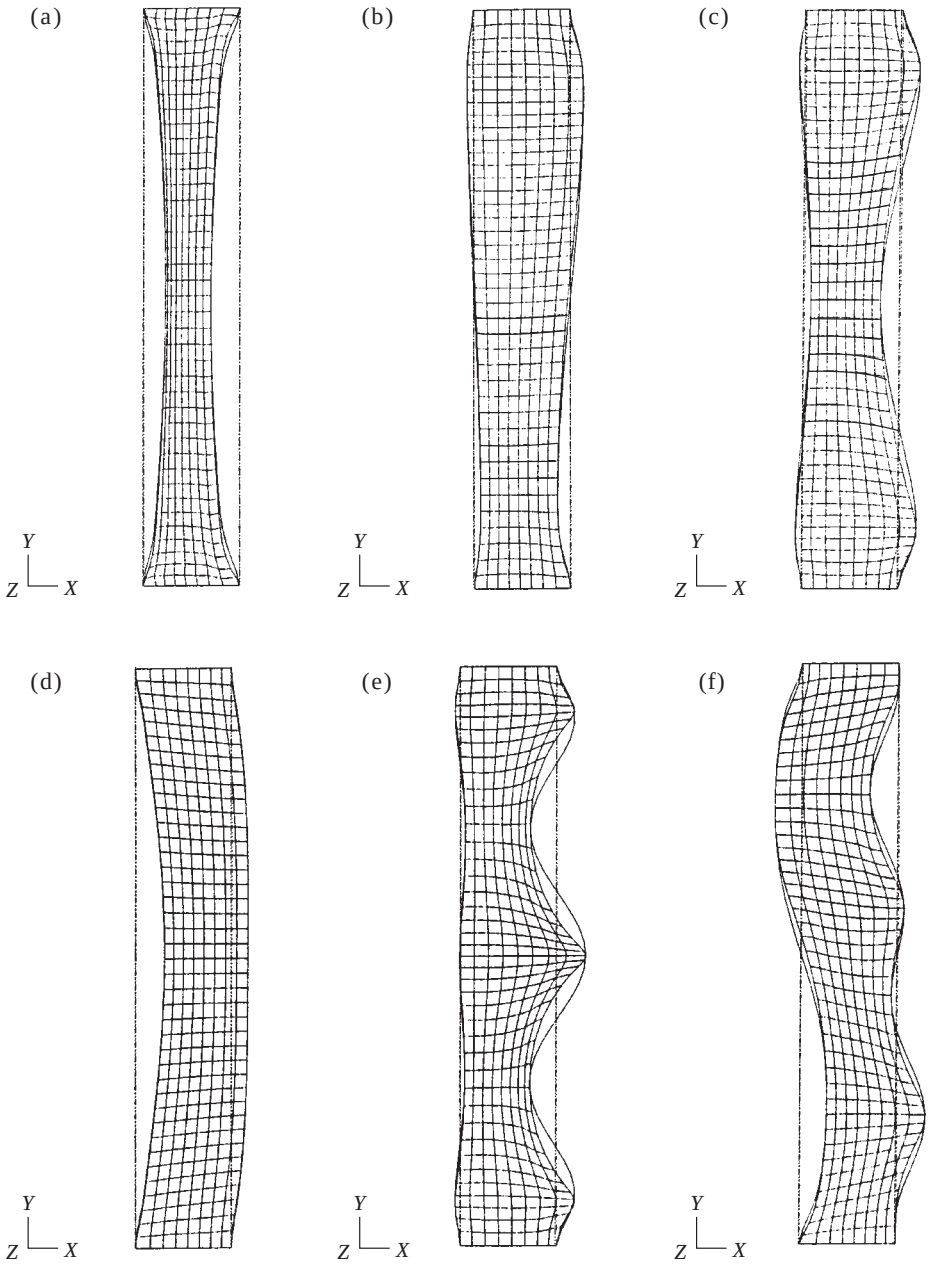

Figure 2. Two-dimensional axisymmetric mode shapes for the circumferential wavenumber $n = 1$. (a) First serial mode (392·0 Hz), $m' = 1$, out-of-phase mode; (b) second serial mode (856·6 Hz), $m' = 2$, out-of-phase mode; (c) third serial mode (1417·8 Hz), $m' = 3$, out-of-phase mode; (d) fourth serial mode (1735·7 Hz), $m' = 1$, in-phase mode; (e) sixth serial mode (2359·8 Hz), $m' = 5$, out-of-phase mode; (f) seventh serial mode (2609·2 Hz) mixed mode.

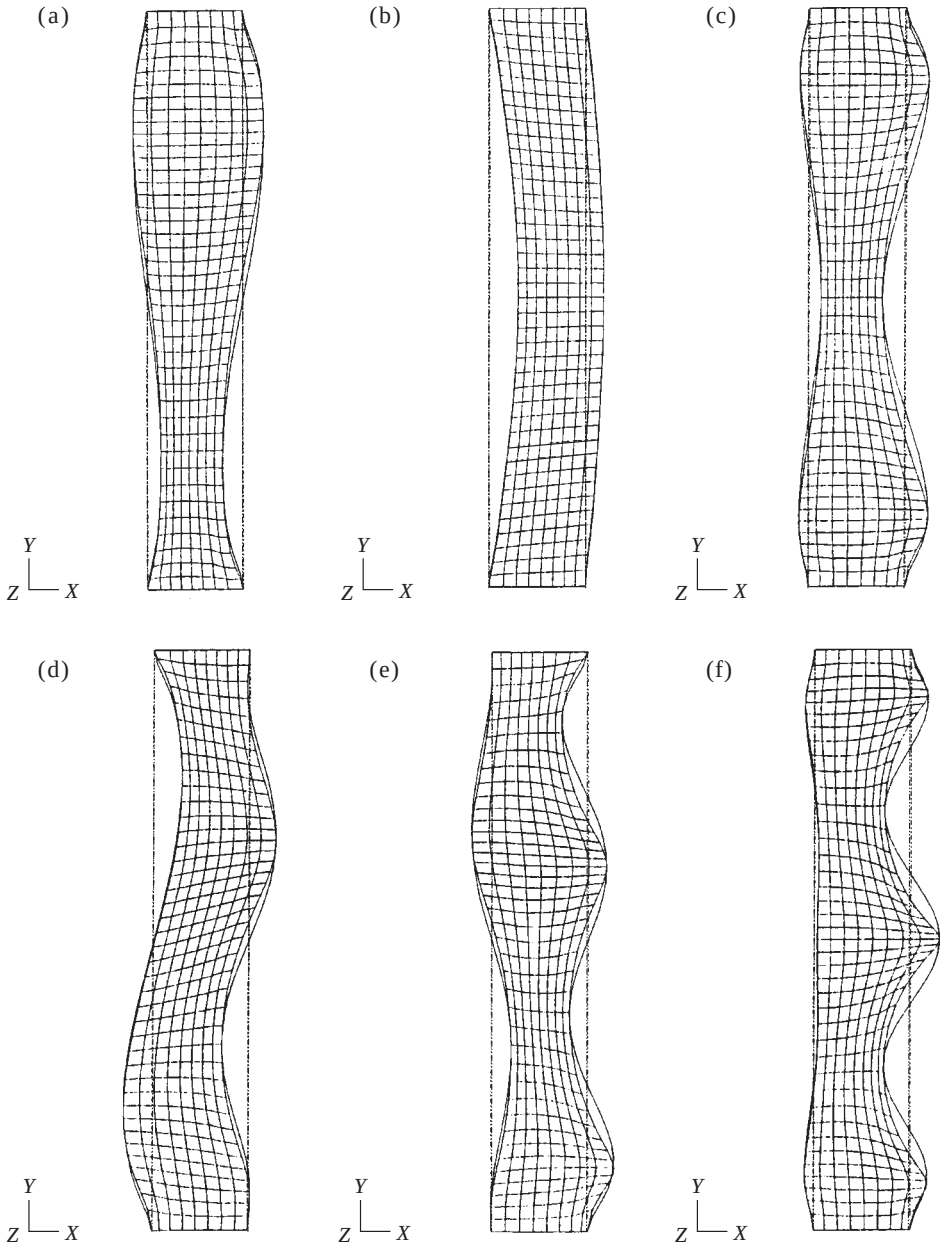

Figure 3. Two-dimensional axisymmetric mode shapes for the circumferential wavenumber $n = 2$. (a) Second serial mode (909·7 Hz), $m' = 2$, out-of-phase mode; (b) third serial mode (994·1 Hz), $m' = 1$, in-phase mode; (c) fourth serial mode (1414·6 Hz), $m' = 3$, out-of-phase mode; (d) fifth serial mode (1828.0 Hz), mixed mode; (e) sixth serial mode (1911.8 Hz), mixed mode; (f) seventh serial mode (2302.1 Hz), mixed mode.

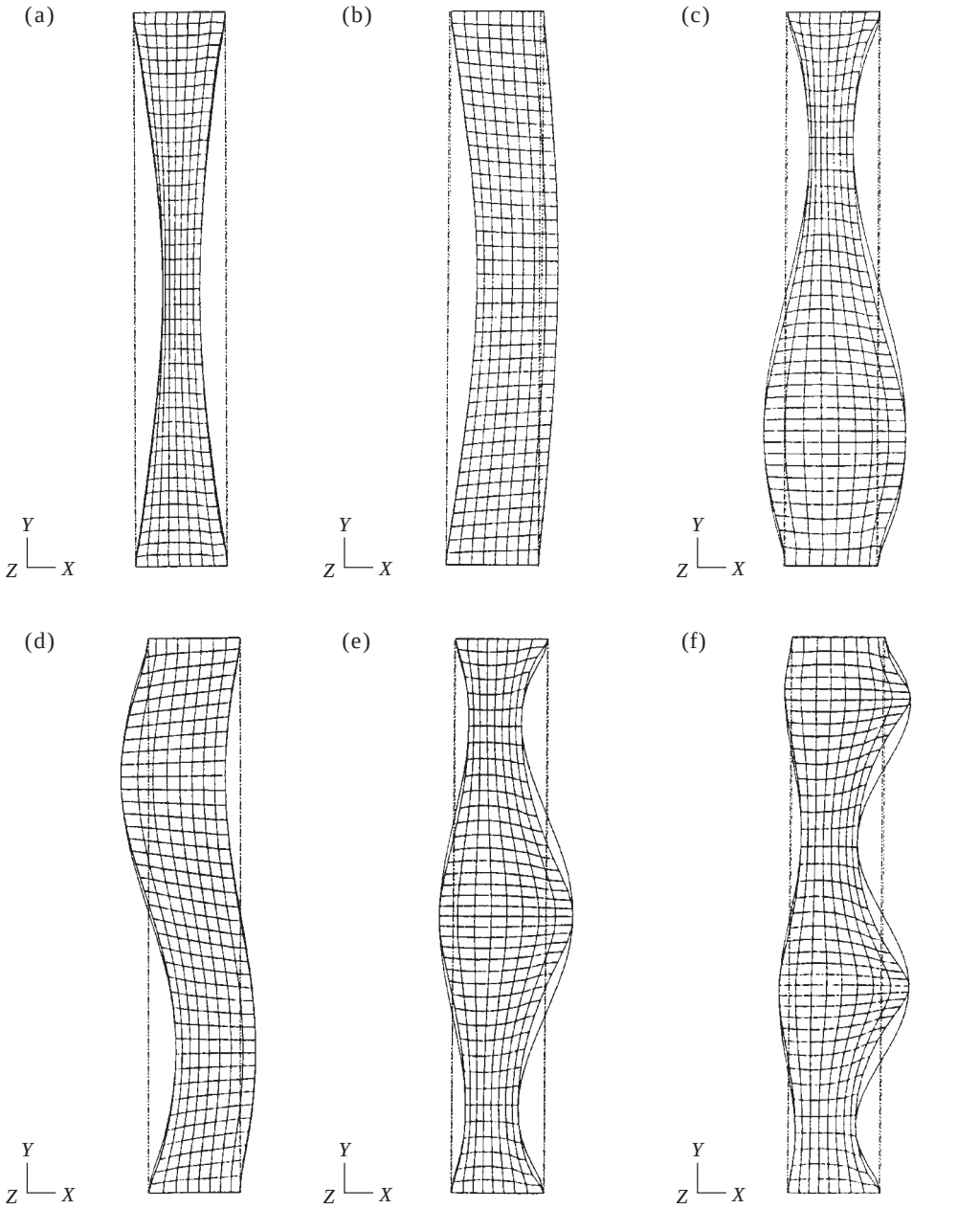

Figure 4. Two-dimensional axisymmetric mode shapes for the circumferential wavenumber $n = 3$. (a) First serial mode (402·2 Hz), $m' = 1$, out-of-phase mode; (b) second serial mode (669.2 Hz), $m' = 1$, in-phase mode; (c) third serial mode (858·3 Hz), $m' = 2$, out-of-phase mode; (d) fourth serial mode (1341· 4 Hz), $m' = 2$, in-phase mode; (e) fifth serial mode (1359·3 Hz), $m' = 3$, out-of-phase mode; (f) sixth serial mode (1829·5 Hz), $m' = 4$, out-of-phase mode.

increases and the annular gap decreases, the coupling effect of fluid will become strong, and the in-phase and out-of-phase modes will appear clearly. On the contrary, when the fluid density decreases or the annular gap increases or the number of modes increases, the ambiguous mixed modes will appear instead of the in-phase and out-of-phase modes. Therefore, strictly speaking, the real in-phase and real out-of-phase modes in the coaxial cylindrical shells coupled with fluid may not exist, but only the serial modes similar to the in-phase and out-of-phase modes may exist. In the strict sense of the word, these modes can be called the apparent in-phase or apparent out-of-phase modes. The low fluid density and the large annular gap in the fluid-coupled system may increase the possibility of the ambiguous mixed mode appearance in the lower frequency range. From this point of view, all of the in-phase, out-of-phase and mixed modes can be interpreted as an appearance of the similar modal pattern from the sequential serial modes.

The first, second and third serial modes of the circumferential mode number $n = 1$ are typical apparent out-of-phase modes, as shown in Figure 2. The fourth serial mode of $n = 1$ in Figure 2, third serial mode of $n = 2$ in Figure 3 and fourth mode of $n = 3$ in Figure 4 are the typical apparent in-phase vibrational modes. The seventh serial mode of circumferential mode number $n = 1$ in Figure 2 is a mixed vibrational mode which resembles a mode with the axial mode $m' = 2$ for the inner shell and $m' = 4$ for the outer shell. The mixed mode shows an influence of the inner shell deformation on the mode shape of the outer shell. The fifth serial mode of $n = 2$ in Figure 3 is another mixed mode, similar to the in-phase mode with the axial mode number $m' = 2$. The sixth serial mode of $n = 2$ in Figure 3 is a mixed mode, which resembles an out-of-phase vibrational mode with the axial mode number $m' = 3$ for the inner shell and $m' = 4$ for the outer shell. The seventh serial mode for $n = 2$ in Figure 3 is a mixed mode, which maintains the out-of-phase mode in the top and bottom regions of the shells and keeps the weak in-phase mode in the central region of the shells. Judging from a review of the vibrational mode shapes, as the axial mode number or the serial mode number increases, it is found that the mixed vibrational modes appear frequently. As the circumferential mode number increases, the out-of-phase and in-phase modes in the serial vibrational modes appear alternatively.

4. CONCLUSIONS

An analytical method to estimate the coupled natural frequencies of coaxial cylindrical shells filled with compressible fluid in the annular gap is developed using the series expansion method based on the finite Fourier transform. To clarify the validity of the analytical method, an example for the clamped cylindrical shells is examined using the analytical method and finite element method. Complete agreement is found between them, and the analytical method is verified. All possible natural frequencies of the fluid-filled coaxial cylindrical shells, not only for the in-phase and out-of-phase modes, but also for the ambiguous mixed modes, can be obtained.

REFERENCES

1. D. Krajcinovic 1974 *Nuclear Engineering and Design* **30**, 242–248. Vibration of two coaxial cylindrical shells containing fluids.
2. S. S. Chen and G. S. Rosenberg 1975 *Nuclear Engineering and Design* **32**, 302–310. Dynamics of a coupled shell–fluid system.
3. M. K. Au-Yang 1975 *NPGD-TM*-320, Babcock & Wilcox. Free vibration of fluid-coupled coaxial cylinders of different lengths.
4. T. Chiba and N. Kobayashi 1983 7*th SMiRT*, 507–514. A comparison of experimental and theoretical vibration results for fluid-coupled, coaxial cylinder.

5. J. TANI, K. OTOMO, T. SAKAI and M. CHIBA 1989 *Sloshing and Fluid–Structure Vibration*—1989, *PVP*, **157**, 29–34. Hydroelastic vibration of partially liquid-filled coaxial cylindrical shells.
6. S. YOSHIKAWA, E. G. WILLIAMS and K. B. WASHBURN 1994 *Journal of Acoustic Society of America* **95**, 3273–3286. Vibration of two concentric submerged cylindrical shells coupled by the entrained fluid.
7. T. R. KIM *et al*. 1992 *KAERI/RR*-1162/92. Korea Atomic Energy Research Institute. A study on the change in dynamic characteristics of reactor internals (in Korean).
8. K. H. JEONG and S. C. LEE 1996 *Computers & Structures* **58**, 937–946. Fourier series expansion method for free vibration analysis of either a partially liquid-filled or a partially liquid-surrounded circular cylindrical shell.
9. I. N. SNEDDON 1951 *Fourier Transforms*. New York: McGraw-Hill Book.
10. S. S. CHEN 1987 *Flow-Induced Vibration of Circular Cylindrical Structures*. Washington, DC: Hemisphere. Publishing Corperation.

APPENDIX: NOMENCLATURE

A_{mnj} Fourier coefficients related to modal function in axial direction
a_{ij} derived coefficients in equation (22)
B_{mnj} Fourier coefficients related to modal function in azimuthal direction
B bulk modulus of elasticity of fluid
c speed of sound in fluid medium
c_{ik} derived coefficients in equation (30)
C_{mnj} Fourier coefficients related to modal function in radial direction
D $Eh/(1-\mu^2)$
D_{onj} Fourier coefficients related to fluid motion
D_{mnj} Fourier coefficients related to fluid motion
d_{ij} derived coefficients in equation (22)
E Young's modulus of shells
e_{ik} derived coefficients in equation (30)
f_{ij} derived coefficients in equation (24)
$f(x)$ spacial velocity potential in axial direction defined in equation (8)
G_{onj} derived coefficients in equation (19)
G_{mnj} derived coefficients in equation (19)
g_{ij} derived coefficients in equation (25)
i $\sqrt{-1}$
$[H]$ column matrix defined in equation (31)
h thickness of cylindrical shells
K $Eh^3/12(1-\mu^2)$
k_j $h^2/12R_j^2$
m Fourier components in axial direction
m' axial mode number
M_{xj} bending moment per unit length
$N_{x\theta j}$ effective membrane shear force per unit length
N_{xj} membrane force per unit length
n circumferential wavenumber
L height of shells
p_j dynamic liquid pressures on the inner and outer shells
Q_{xj} effective transverse shear force per unit length
q_{ij} derived coefficients in equations (20) and (21)
r radial co-ordinate
t time
u_j axial dynamic displacements of shells
v_j tangential dynamic displacements of shells
w_j radial dynamic displacements of shells
x axial co-ordinate
α_{mn} defined in equation (11)
β_{ij} derived coefficients in equations (27a) and (27b)
γ_j^2 $\rho R_j^2(1-\mu^2)/E$
δ_j 1 for the subscript $j=1$ and -1 for $j=2$ in equations (18) and (19)

δ_{ij} derived coefficients in equation (27c) and (27d)
Γ_{onj} derived coefficients in equation (19)
Γ_{mnj} derived coefficients in equation (19)
$[\zeta]$ derived coefficients in 8×6 matrix equation (28)
η velocity potential function of r and θ
θ tangential co-ordinate
μ Poisson's ratio
ρ density of cylindrical shells
ρ_o density of fluid
Φ general velocity potential function of r, θ, x and t
ϕ spacial velocity potential function of r, θ and x
ω coupled natural frequency